Unraveling the role of sintering temperature on physical, structural and tribological characteristics of ball milled Co28Cr6Mo biomaterial based alloy

Mohammed FARAH, Mamoun FELLAH, Dikra BOURAS, Naouel HEZIL, Abderrachid BECHERI, Barille REGIS, i Henda DAOUD, Alex MONTAGNE, Tmader ALBALLA, Hamiden ABD EL-WAHED KHALIFA

PII: S2307-1877(23)00301-2

DOI: https://doi.org/10.1016/j.jer.2023.10.040

Reference: JER100273

To appear in: *Journal of Engineering Research*

Received date: 14 April 2023
Revised date: 15 October 2023
Accepted date: 30 October 2023

Please cite this article as: Mohammed FARAH, Mamoun FELLAH, Dikra BOURAS, Naouel HEZIL, Abderrachid BECHERI, Barille REGIS, i Henda DAOUD, Alex MONTAGNE, Tmader ALBALLA and Hamiden ABD EL-WAHED KHALIFA, Unraveling the role of sintering temperature on physical, structural and tribological characteristics of ball milled Co28Cr6Mo biomaterial based alloy, *Journal of Engineering Research,* (2023) doi:https://doi.org/10.1016/j.jer.2023.10.040

Unraveling the role of sintering temperature on physical, structural and tribological characteristics of ball milled Co28Cr6Mo biomaterial based alloy

Mohammed FARAH[1*], Mamoun FELLAH[2,3*], Dikra BOURAS[4], Naouel HEZIL[3,5], Abderrachid BECHERI [1], Barille REGIS [6], i Henda DAOUD[7], Alex MONTAGNE[8], Tmader ALBALLA[9], Hamiden ABD EL-WAHED KHALIFA[10,11]

[1]Matter Sciences Department, Faculty of exact Sciences and Natural and Life sciences, Echahid Cheikh Larbi Tebessi University – Tebessa, 12000Algeria
[2]Mechanical Engineering Department, ABBES Laghrour-University, Khenchela, P.O 1252, 40004, Algeria.
[3] Research team, Biomaterial, synthesis and tribology, ABBES Laghrour-University, Khenchela, P.O 1252, 40004
[4]Faculty of Science and Technology, University of Souk-Ahras, Algeria
[5]Matter Sciences Department, ABBES Laghrour – University, Khenchela P.O 1252, 40004, Algeria

[6] MOLTECH-Anjou, Universitéd'Angers/UMR CNRS 6200, 2 Bd Lavoisier, 49045 Angers, France.

[7]Higher institue of biotechnology of Monestir, P.O74, 5000, Monestire, Tunisia
[8]LAMIH Univ Polytechnique Hauts-de-France, UMR 8201 -F-59313 Valenciennes, France
[9]Department of mathematics, College of Sciences, Princess Nourah bint Abdulrahman university, P/O. Box 84428, Riyadh 11671, Saudi Arabia
[10]Departement of Mathematics, College of Science and Arts, Qassim University Al-Badaya 51951, Saudi Arabia
[11]Departement of operations and Management research, Faculty of graduate studies for statical research, Cairo University, Giza 12613; Egypt
*Corresponding author: mohammed.farah@univ-tebessa.dz ; mamoune.fellah@univ-khenchela.dz

ABSTRACT

This work aim to investigate the effect of sintering temperature (950 to 1250 °C) on structural, physical, tribological properties of nanobiomaterial Co28Cr6Mo alloy for total hip prosthesis obtained by high Energy ball milled. Several techniques such as density, porosity, microhardness, and Young's modulus were used to assess the mechanical and physical characteristics.
Tribological behavior were conducted using a ball-on-plate type Oscillating tribometer, under different applied loads (2, 10 and 20 N), under a wet condition using hank's solution to simulate human body fluid.

SEM, EDS and XRD analysis results, showed that Co-Cr-Mo alloy samples sintered exhibit the same phases created by the Co element. The alloy sintered at 1250 °C displayed the highest micro-hardness value in terms of mechanical characteristics (386.75 $HV_{0.1.}$ The porosity changes from 17 % to 10 % and endorse a higher change in Young's modulus around 61.84 and 92.5 GPa for samples sintered beteew 950 and 1250°C, respectively,. A remarkable decrease in the wear rate and volume values is obtained for the sample sintered at 1250 °C (32.1610-3 μm3 (N.m)-1) compared to other samples sintered at 1150 and 1250°C. Under wet tribological conditions, the abrasive and adhesive wear mechanisms were identified as the main degradation mechanisms for all sintered samples.

Keywords: CoCrMo alloy; Sintering; Porosity; Tribology; Biomaterials; Nanoparticles.

INTRODUCTION

The improvement of biomaterials has made possible to enhance the protection and residing comfort of people with practical deficiencies (Stojanović et al., 2019, Shekhawat et al., 2021 & Liu et al., 2017). However, up to date, a lot of challenges are required to be faced to strengthen the application of biomaterials based alloys in bone tissue. Of this, the response of body transplants is considered as a matter in clinical research studies. This reaction is not always favorable because of the many issues that could arise after transplantation (Igual et al., 2019 & Yildirim et al., 2019)

Numerous medical and scientific studies focus on distinguishing types of stresses that are involved in the biomaterial degradation. Among them, mechanical associated with friction, corrosion and ground fatigue problems (Fellah et al., 2019). The last can simultaneously produce corrosion particles and breaks inside transfers and consequently the metal ions dissolution in the human body. All of those interactions are probability will lead to generous inflammatory reactions (Taghian Dehaghani et al., 2015). While the physical and chemical stresses result in the presence of many ions along with chlorides, phosphates, sodium cations, potassium and oxygen in fluids and cells in contact with the metal implants actually have a enormous effect at the corrosion behavior (Roudnicka et al., 2021 & Lizárraga et al., 2017).

Along with metal implants, cobalt-based alloys are biomaterials of immense scientific and technological interest. In particular, CoCrMo alloys have shown great mechanical properties, corrosion resistance and a high biocompatibility with human tissues (Yamanaka et al., 2014). CoCrMo alloys are used as orthopedic implants, to stabilize bones, intervertebral discs, dental appliances, and as help structures for coronary heart valves (Fellah et al., 2023) Cobalt-chromium alloys are historically fabricated by means of many production strategies consisting of casting and conventional consistent with ASTM-F75 (Yoda et al., 2012). These techniques have defects in rude microstructure, energy and elongation to rupture, due to defects in rigidity, and flaking (Sinnett-Jones et al., 2005).

One of the most important drawbacks of these alloys is the difference among Young's modulus (210 GPa) and bone's modulus (30 GPa), which causes the phenomenon of fatigue safety (Yamanaka et

al., 2012 & Fellah et al., 2014). The use of porous materials is a way to fix up this troubles. By adjusting the implant porosity, the hardness can be reduced to fit natural bone (Fellah et al. 2019).

In order to keep away from revisions, a strong demand is needed to enhance the overall performance of CoCrMo alloys. For this challenge, one of the applicable techniques for producing this alloy is powder metallurgy. Sintering has been typically used to make alloys of excessive purity, with centered chemical compositions, ideal structures and controlled porosity. (Yamanaka et al., 2012). This work focuses on the synthesis of a CoCrMo-type cobalt-based alloy for medical applications using ball milling method. Cobalt-chromium alloys are among the most commonly used biomaterials so far in implants due to their excellent resistance to corrosion and wear. Friction and corrosion of these materials in a corrosive environment are key parameters to study in order to extend their life. (Shekhawat et al., 2021 & Roudnicka et al., 2021). The addition of chromium improves the corrosion resistance due to the spontaneous formation of a protective passive layer, formed mainly of chromium oxide. The addition of molybdenum makes it possible to produce finer grains, and reinforces the resistance to localized corrosion in chloride environments. To obtain CoCrMo-type cobalt-based metal alloy with required characteristics, the effect of sintering temperature was thoroughly investigated on the structural, physical and also tribological characteristics.

MATERIALS AND METHODS

Preparation of the alloys

Elemental powders of Co, Cr, Mo, (Fig. 1) were purchased from Sigma Aldrich Chemicals Ltd and were used to synthesize Co-28Cr-6Mo alloy. Table 1 below shows the characteristics of the elementary powders. The alloy was synthesized by mixing the desired amounts of elemental powders: Co (balnce), (28 at.%) Cr and (6.at.%) Mo to get Co28Cr6Mo alloy, and then the mixture was ball milled using high energy ball mill (Fritsch P7) under a protected argon atmosphere.

Table 1 Characteristics of as-received elementary Co, Cr, Mo powders (Fellah et al. 2023)

Element	Co	Cr	Mo
Mean Grain size (µm)	<140	<140	<140
Purity (%)	99.97	99.7	99.8
Shape	Irregular/Spherical	Irregular/Spherical	Irregular/spherical
Melting point (°C)	1492±5	1855±5	2616±5

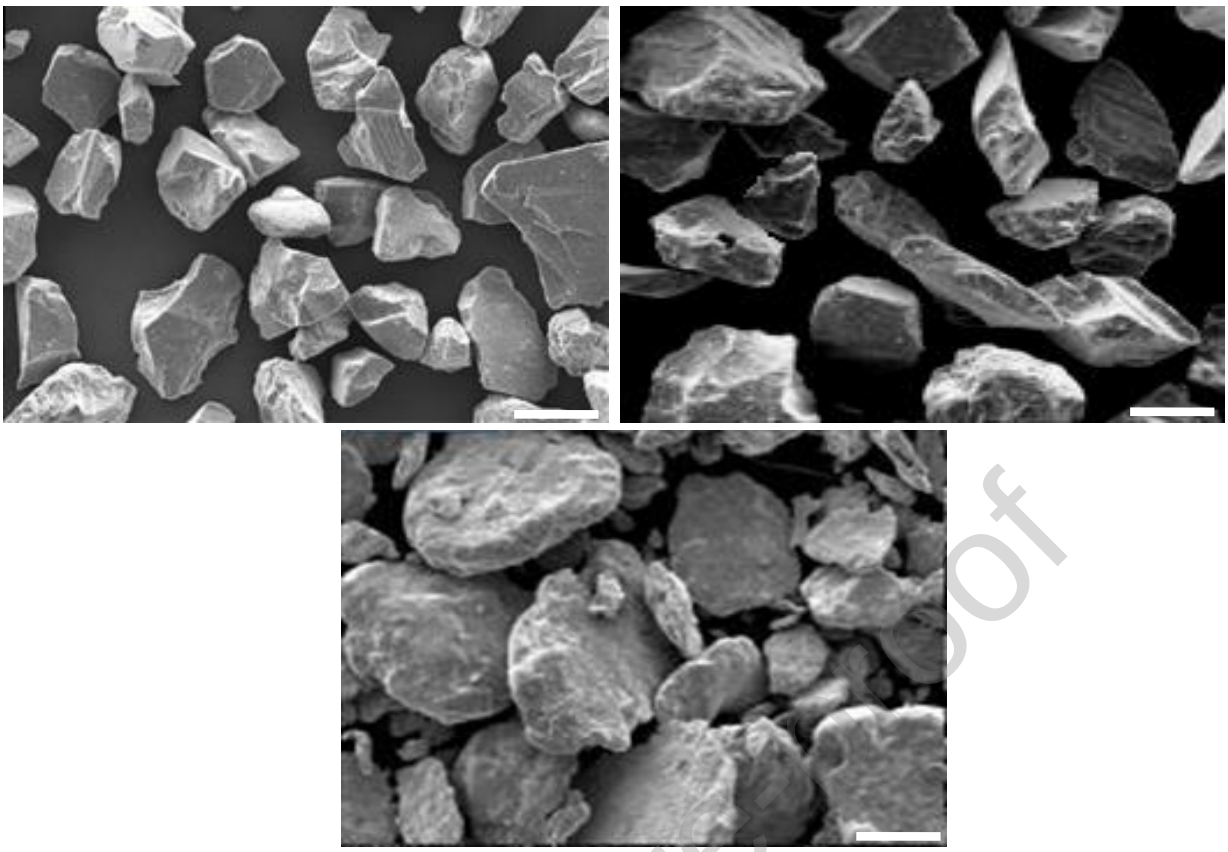

Figure 1. The SEM images of the as received elemental powders (a)-Co, (b)-Cr and (c)-Mo used in the synthesis procedure

The milling medium was mainly composed of 10 mm diameter alumina balls in an 80 mL capacity vial, using a ball-to-powder ratio of 20:1, for 18 hours. Milling process was performed for 28-minute cycles with a 9-minute rest period in between. After each milling cycle, the vials were opened after a 35 to 40 min cooling period in order to avoid excessive heating of the powders caused by repetitive collisions (Fig. 2), Subsequently, the pre-alloyed powders were subjected to a powder metallurgy procedure using both cold and hot pressing. During cold pressing, the mechanically alloyed powders were loaded into the rigid steel die and uniaxially compressed at a pressure of 150 MPa using a manual hydraulic press (Specac 25 Ton), forming a cylindrical shape with 13 mm diameter and 4 mm thickness. After the cold pressing step, the specimens were processed by hot isostatic pressing (HIPing) at a temperature of 1000°C and a pressure of 400 MPa , with 45 min of holding time (Fig. 2).

The HIPed samples were finally sintered, at different temperatures of 950, 1050, 1150 and 1250 °C in a protected atmosphere, with a heating and a cooling rate of 15°C/min and 20 °C/min respectively, at holding time of 3 h. The sintering heat treatment cycle is summarized in Figure 3

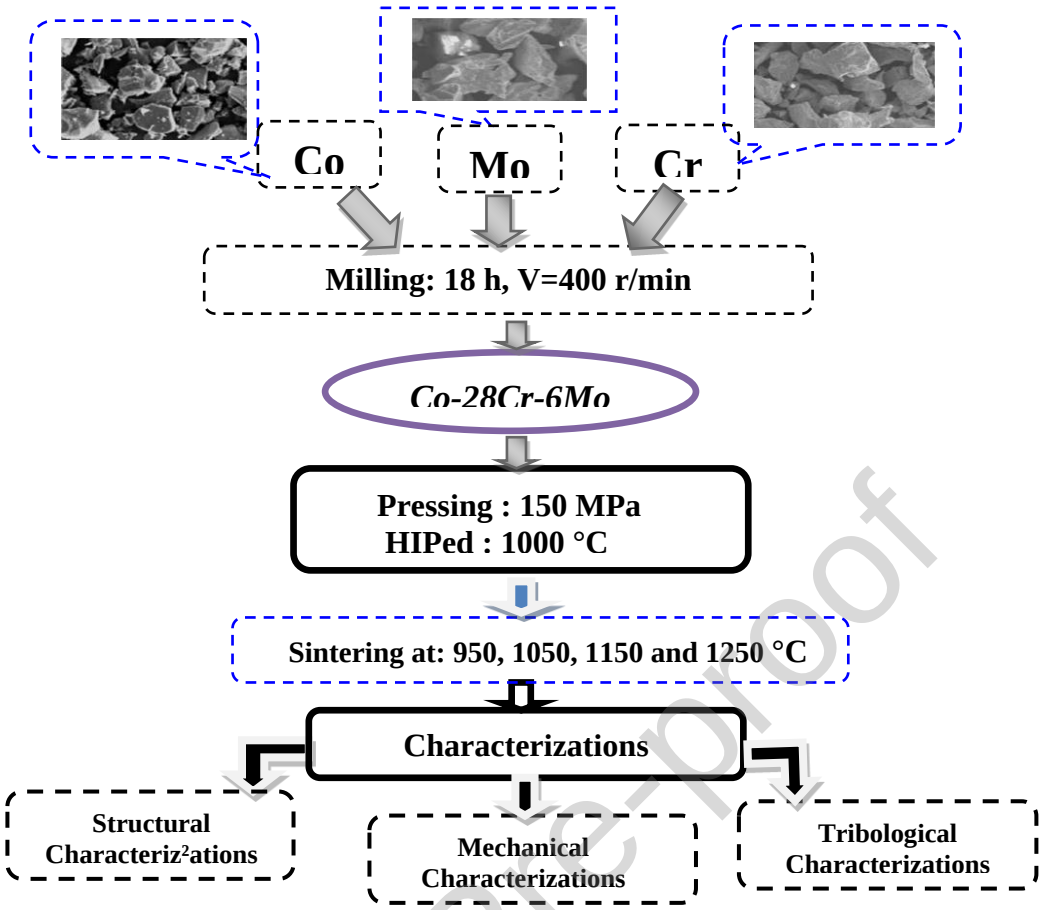

Figure 2. Co28Cr6Mo Samples reparation method

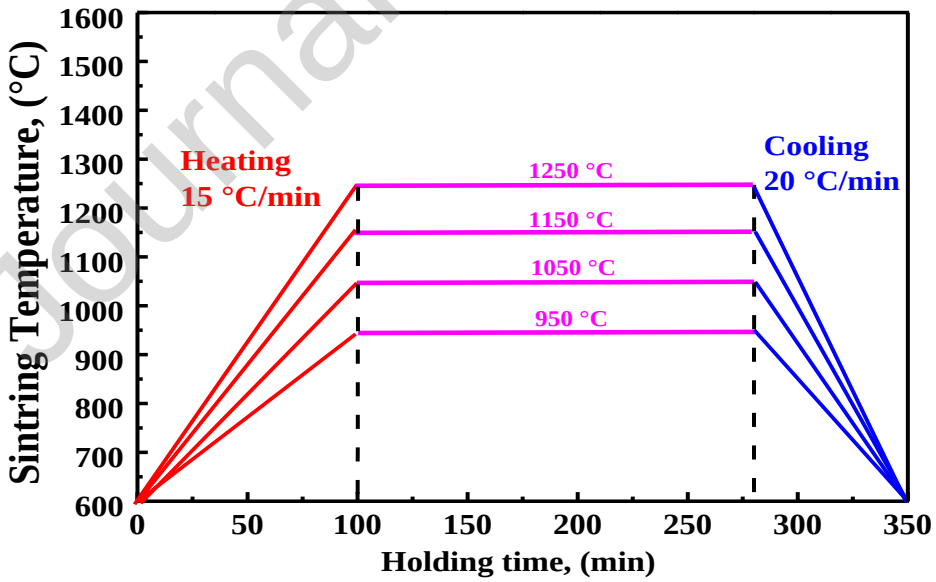

Figure 3. The sintering Heat Treatment Cycle of compacted Co28Cr6Mo Alloys.

2.2 Samples characterization

2.2.1. Structural and mechanical characterization

Structural characterization was performed using Scanning Electron Microscopy (SEM type Hitachi S-520) and X-Ray diffraction Analysis using (XRD type *INTEL CPS 120*/*Brucker AXS)*. SEM was used for investigating the powders morphology, and for analyzing the wear mechanisms, track and debris morphology after the wear tests. XRD was used for structural characterization. SEM analysis was recorded on an accelerating high voltage (HV) of 25 KV.

XRD analysis was performed using a Brucker AXS diffractometer, with a voltage and current values of 40 KV and 20 mA respectively, and a Cu-K_α (λ= 1.5406 Å) radiation using a (<θ>–<2θ>) Bragg-Brentano geometry, along with a scan range of 20 – 110° and a sweep speed of 0.005 °/s in, the phase identification are verified and compared using ASTM codes and standards : ε (Co-hcp) (ICDD:5-727) and γ(Co-fcc)(ICDD:15-806); Mechanical characterizations such as, density, microhardness, porosity, Elastic modulus and roughness were also evaluated. Density was measured utilizing Archimedes' principle (Shukla et al., 2021), while, microhardness and Young's modulus were evaluated using Vickers's microdurometer type *ZwickRoell ZHV10* (ULM, Germany). Pore characteristic parameters were determined by quantitative analysis of micrographs using Image-Pro Plus software" (Fellah et al. 2019)

2.2.2Tribological Characterization

After cold and Hot isostatic pressing and sintering, friction tests were carried out using a Tribotester (TRIBOtechnic type ball-on-disc) as illustrated in Figure 4, according to ISO 7148. All the wear tests were performed under a simulated body fluid medium using Hank's Solution (Corona-Gomez et al., 2021 & Fellah et al. 2023).

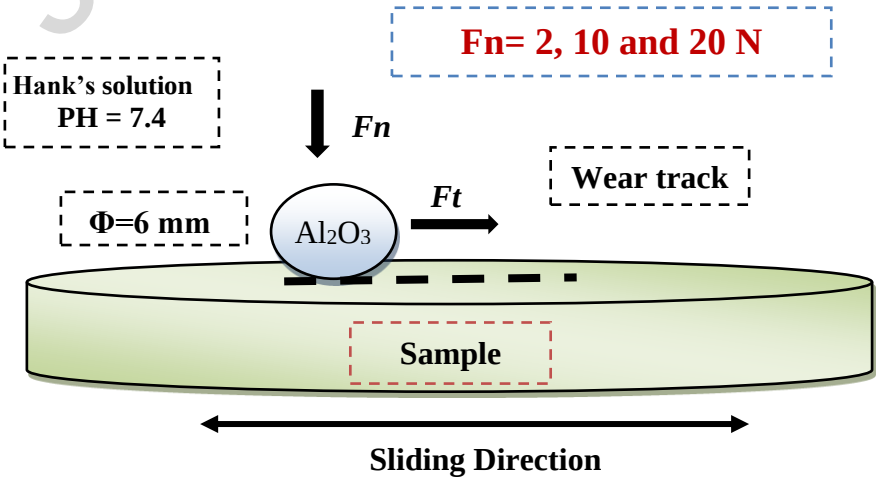

Figure 4. Schema of Tribotester (TRIBOtechnic type ball-on-disc)

RESULTS AND DISCUSSION

Structural characterization

SEM-EDS analysis

. The results demonstrated that the Co segment represents the majority phase which constitutes the grey coloration matrix, with a distribution of areas of dark lamellar morphology rich in chromium and light areas rich in molybdenum. These outcomes are showed by means of the quantitative evaluation of EDS (Table. 2). The experimental conditions used together with the initial composition, the synthesis method, the sintering temperature and time have an influence on the formation and constitution of the phases obtained (Eka Perkasa et al., 2019).

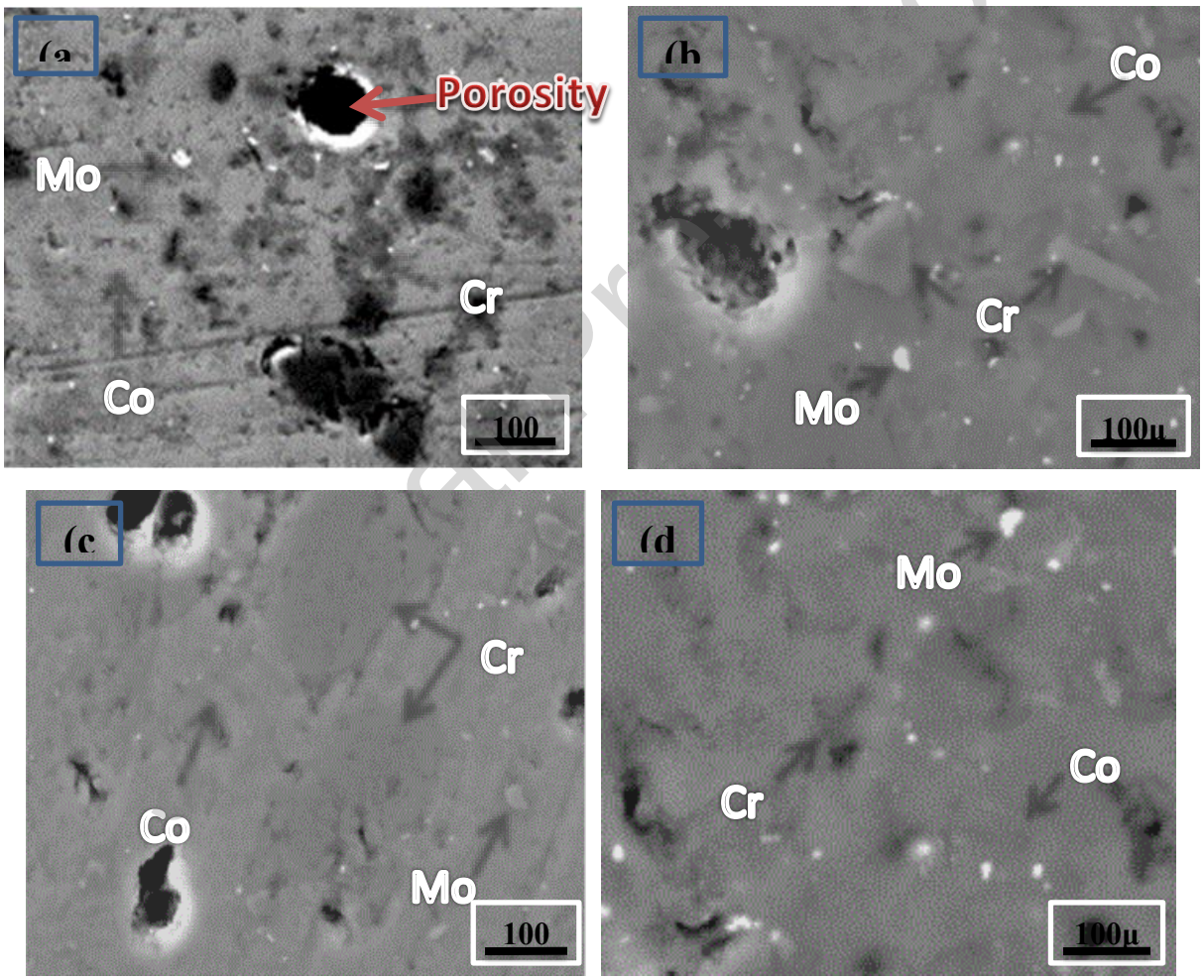

Figure 5. SEM micrographs of the Co28Cr6Mo sample sintered at different temperatures. (a) 950, (b) 1050, (c) 1150 and (d) 1250 °C.

The chemical composition obtained with power dispersive X-ray spectrometry for special phases are depicted in Figure 6. The effects given via the EDS verify that for the matrix (gray region) the existence of cobalt spikes and the analysis of the dark segment suggest the presence of chromium. For the white segment, the evaluation outcomes show molybdenum spikes. No carbide is gift inside

the microstructure, which corresponds adequately to the XRD analysis results of the Co26Cr8Mo alloy given by Figure 7 (Zangeneh et al., 2012).

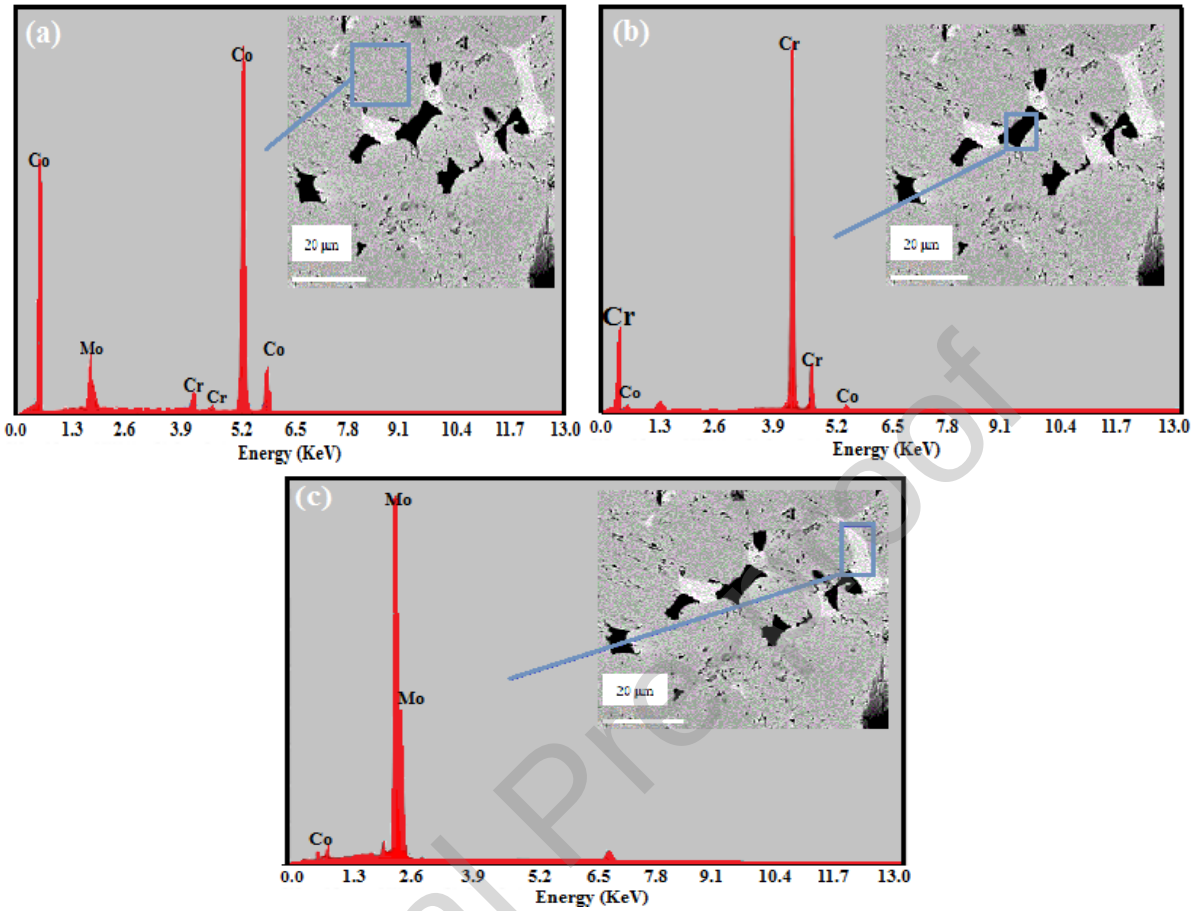

Figure 6 EDS Different spectra of the sintered Co28Cr6Mo at 1250 °C.

Table. 2 EDS spectra of the sintered Co28Cr6Mo alloy.

Sample	Co (at.%)	Cr	Mo	O (at.%)
950 °C	65.4	28.6	4	2
1050 °C	64.1	24.5	8.4	3
1150 °C	59.7	29.6	7.2	3.5
1250 °C	61.4	27.9	6,5	4.2.

X-ray diffraction analysis

XRD patterns recorded on different samples are illustrated in Figure 7. This indexing genuinely suggests the presence of the ε-Co with a compact hexagonal crystal shape (HC), all of the samples heat-treated with the aid of sintering, which confirms the one-section character of the CoCrMo alloy according with what has been published in the literature (Shukla et al., 2021, Eka Perkasa et al., 2019, Fellah et al., 2023). Amore precise analysis of the diffraction peaks of the CoCrMo alloy was carried out for 2Θ values ranging from 25° to 95°.

To sudy the evolution of each phases after treatment, only the diffraction peaks of the planes (011) (022), (122) for the γ-Co phase (fcc) : (ICDD:15-806) and those of planes (101), (102), (100), (102) of the ε-Co phase (hcp) (ICDD:5-727) were used. These diffraction planes have higher intensities, which reduces the margins of error when calculating the volume proportions of phases present in the Co28Cr6Mo (Saldívar-García et al., 2005). No look of recent peaks of the alternative levels formed together with the σ phase in the CoCr phases and the intermetallic phases within the Co-Mo system had been located t the diffractograms of the sintered alloy at exceptional temperatures (Fellah et al., 2020).

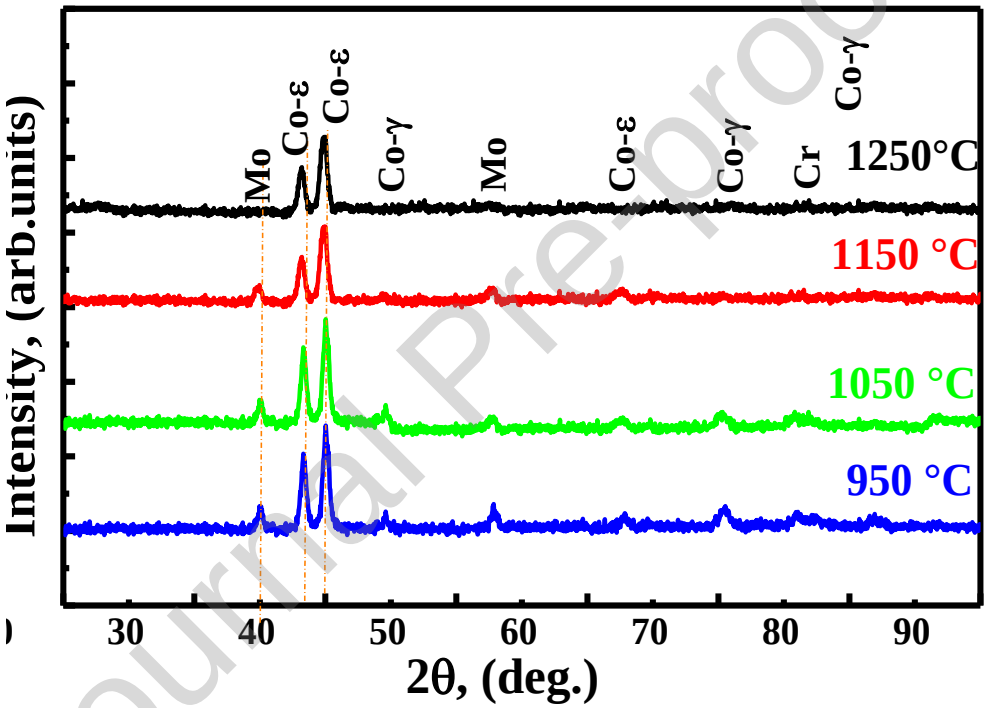

Figure 7. XRD diffraction spectra of the sintered Co28Cr6Mo alloy at different temperatures

This result is not associated to non-lifestyles of these levels in as-prepared samples, however it may be explained by means of the small amount of these stages at some point of the sintering, which gives very susceptible diffraction peaks which can be tough to differentiate because of past noise which is very important in our diffraction diagrams (Hezil et . al 2019, Namus et al., 2020, & Bouras et al. 2023)

Crystallite size and microstrain

The evolution of the average crystallite-size “D” (nm) and the internal microstrain values Ɛ (%) of CoCrMo alloy sintered at different temperatures are displayed in Figure 8. The crystallites size

was determined by the broadening of the diffraction peaks within ± 5 nm accuracy using Scherer formula, While lattice strain was determined using the classical Williamson–Hall, (W–H) equation (Fellah et al., 2023 & Hammadi et al.2021):

$$D = \frac{k\lambda}{\beta \cos\theta} \quad \text{(Eq.1)} \qquad \text{and} \qquad \varepsilon = (\beta\cos\Theta/4\sin\Theta)-(\frac{K\lambda}{4D\sin\Theta}) \quad \text{(Eq.2)}$$

where D is the average crystallites size of the ordered domains, β is the full width at half maximum (FWHM) of peaks, k is a dimensionless shape factor (~1.0), ε is a lattice distortion (microstrain), λ is the wavelength of the X-ray and θ is the Bragg angle. Grain size growth in addition to the relaxation and release of micro-stresses that are induced in the crystal lattice by the annihilation of various structural defects.

It can be clearly seen that the crystallite size gradually increases with increasing sintering temperature, staring from 11.55 nm at 950 °C and reaching a value of 15.53 nm at 1250 °C. This increase may be due to the expansion of the stresses introduced under the effect of the sintering temperature which is in accordance with the displacement of the peaks towards smaller angles.

The evolution of microstrain <ε> (%) it rapidly decreases as a function of sintering temperature from 950 to 1250 °C with values of 0.0893 to 0.0722 %, respectively. This can be attributed to the stacking defects and the density of dislocations caused by the plastic deformations sustained by the particles, grain surface relaxation and most importantly to lattice distortion caused by phase transformation (Ren et al., 2016 et Fellah et al., 2019). Furthermore, the transformation has entered the stabilization phase and further phase transformation is not possible, since the Co28Cr6Mo alloy is completely formed. The alloying elements Cr and Mo were completely inserted in the Co matrix forming the final HCp phase. The above observations and results can be attributed to the refinement of particle size, up to the nanosized scale followed by an increase in the micro strains induced at the internal level

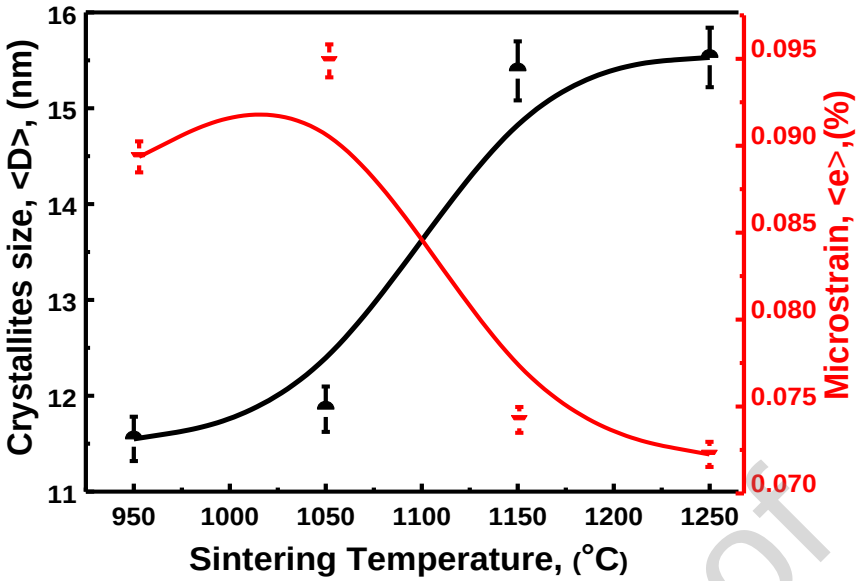

Figure 8. The evolution of microstrain <*ε*> *(%)* and crystallites size <*D*> *(nm)* as a function of sintering temperature.

Mechanical characterization

Density and porosity

Biomedical materials require a positive qualification of porosity. Pores are necessary for tissue formation, as they permit cell migration and proliferation, in addition to vascularization (Yamanaka et al., 2014). We consequently hold that sintering at a high temperature has a fine effect on the reduction of porosity and the boom of hardness. It is well known that the mechanical properties and the microstructure of sintered Co28Cr6Mo alloy are strongly stimulated through the heat treatment (sintering) parameters, particularly the sintering temperature (Saldívar-García et al., 2005 & Namus et al., 2020).

The material becomes compact for a temperature of 1250 °C, taking into account the melting temperature of the base element cobalt (1490 °C), sintering at 1250 °C ensures healing of the bridges following an extreme viscous waft of rely. The densification mechanisms involved in the course of sintering are specifically extent diffusion among debris of the equal nature (unmarried-segment sintering) and the viscous flow of the debris underneath the impact of temperature (Cuao-Moreu et al., 2019). Approaching the melting point of the least refractory section, the viscous glide of the particles is considerably accelerated, ensuing in a closure of the pores by using displacement of the bridges among the substances. When sintering is achieved a temperature of 950 °C, the relative porosity is of around 17 %, therefore a low hardness.

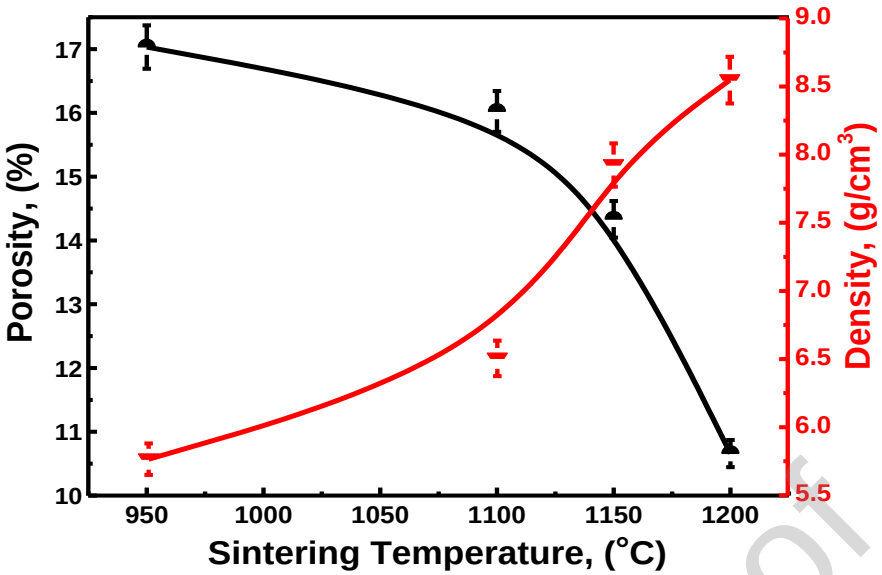

Figure 9. Evolution of the density and the porosity of the Co28Cr6Mo samples as a function of the sintering temperature.

Figure 9 summarizes the density and porosity of the samples sintered at different temperatures. It is observed that the passage of the sintering temperature from 950 to 1250 °C is accompanied by means of a non-negligible increase inside the density and decrease within the porosity. As the sintering temperature decreases, it seems that the density is strongly decreased with increasing of porosity (Toh et al., 2017).

Microhardness and Young's modulus

Microhardness is a critical feature for metallic materials meant for biomedical programs, mainly because of the friction troubles of clinical prostheses. This friction releases alloy particles that can be harmful to the frame (Wei et al., 2018). In this work, the microhardness analysis was carried out to highlight the effect of the sintering temperature and to recognize the effect of the porosity fee on the mechanical properties of the produced Co28Cr6Mo alloy. Based on the obtained results, it can be concluded that the sintering temperature has a crucial effect on the dispersion of the values of the microhardness which indicates that the footprint modifications appreciably when passing from one region to any other (Thornley et al., 2020).

Figure 10 represents the evolution of Young's modulus and microhardness as a function. These two properties increase with increasing sintering temperature, such that the high value of Young's modulus received become 92.44 GPa and the microhardness 386.747 HV for the sample sintered at

1250 °C. The Young's modulus values received are too lower than those published in many research (Ren et al., 2016), which can be of the order of (210-250 GPa).

However, the Young's modulus values obtained are: E = 61.84, 70.6 GPa, 84.4 GPa, 92.5 GPa for samples sintered at 950°C, 1050 °C, 1150 °C, 1250 °C, respectively. Stay encouraging despite the fact that still some distance from that of bone (E = 30 GPa), but although have a much decrease fee than that of the alloys currently used inside the manufacture of prostheses (Cuao-Moreu et al., 2019 & Toh et al., 2017,).

We consequently observe the significant decrease of young's modulus of sintered samples, with the presence of a porosity permitting better mechanical compatibility with the bone, i.e. a reduction within the phenomena pressure-defensive, due to the distinction between the young's modulus of stable implants and bone (Wei et al., 2018, Thornley et al., 2020, Gong et al., 2018 & Kumagai et al., 2006). In addition, the development of the mechanical resistance is the main objective of many research to develop substances having each a low young's modulus of elasticity and a high resistance. According to the outcomes acquired from the young's modulus and microhardness, the CoCrMo alloy has superior residences to cortical bone. It can consequently be concluded that the porous structures lower these properties.

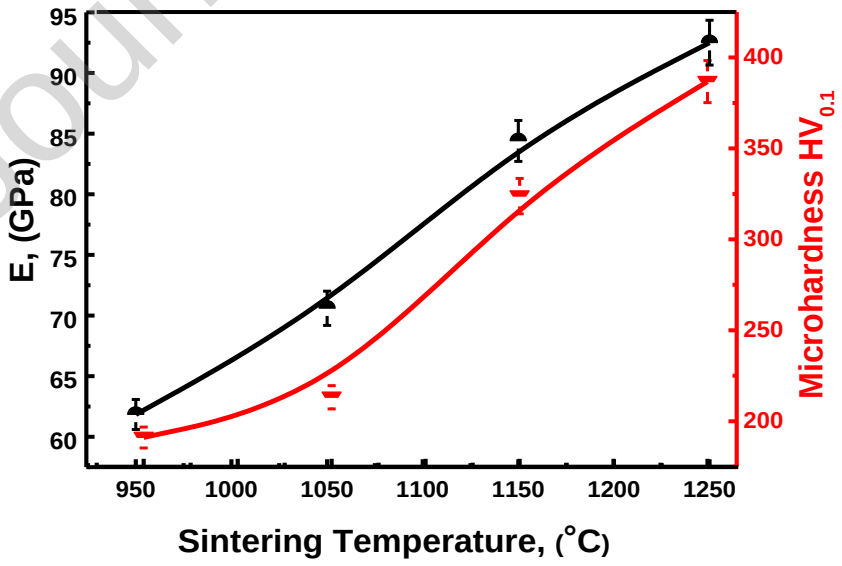

Figure 10. Evolution of microhardness and Young's modulus of Co28Cr6Mo samples sintered at different temperatures

The final result of the microhardness of sintered samples is much better as compared to previous studies, such as those of samples designed by paintings (Eka Perkasa et al., 2019 & Zangeneh et al., 2012). Concerning the evolution of the porosity, the best rate is received for the pattern sintered at 1050 °C. According to the Hall-Petch relationship, the Young's moduls and microhardness increases with a decrease in grain size. microhardness is an important tool for defining the mechanical properties related to microstructure"

Tribological behavior

Coefficient of Friction

The effect of sintering temperature on the tribological behavior of the (Co28Cr6Mo/Al_2O3) was studied under wet conditions simulating the human body fluid using Hank's solution. The deterioration of the cobalt-alloy implants is due to wear, corrosion and their synergistic effect as a result of the simultaneous effect of chemical and mechanical effects in the trabecular contact (Stojanović et al., 2019). For this reason, simulated body fluids have been widely used for many decades to test the tribological properties of biomaterials (Lashgari et al., 2011). In most cases, mineral substances are naturally covered by a negative film when immersed in physiological media. The mechanical action of friction will destroy this protective layer during the coupling of these different mechanisms (Zangeneh et al., 2018).

The friction coefficient shows a decrease with increasing load and sintering temperature in Figure 11. When the load decreases, the projections are compressed and thus subject to flexible plastic deformation. The original point of contact also becomes in contact with the surface, which is equivalent to changing the bump from the plow to friction, indicating a decrease in the friction coefficient. However, it increases with the increase in the applied load. Meanwhile, when the sintering temperature increases and the material contact interface loosen and the microhardness increases. Thus, The above results suggest that the sliding friction of Cr28Co6Mo alloys does not only depend on the sintering temperature, but also depends on the microstructure, and the experimental paramaters such as, applied load, sliding speed, testing environment, friction couple, etc. Thus the coefficient of friction decreases as observed in previous studies (Cheng et al., 2022).

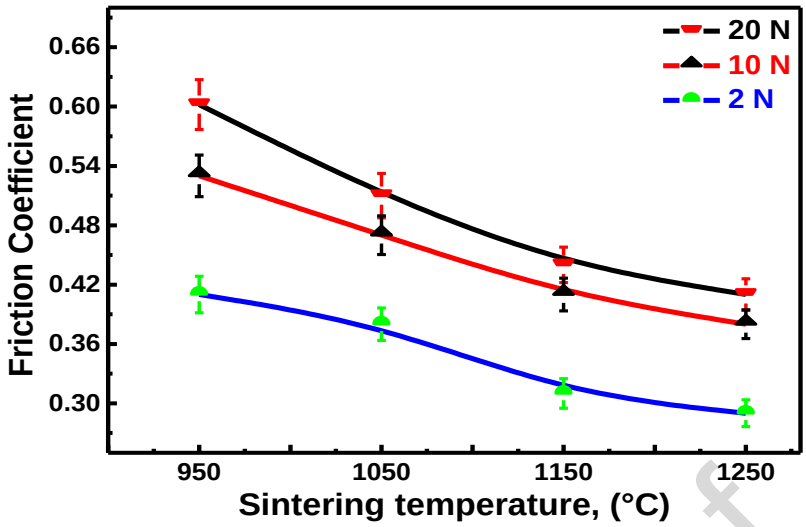

Figure 11. Friction coefficient values of Co-28Cr-6Nb samples as function of sintering temperature.

Wear volume and rate

The wear phenomenon results in a surface degradation in contact by friction during use. Several methods allow us to quantify the wear of the materials tested. In our case we quantified the wear by calculating the wear volume of the cross section of the wear tracks after each friction test (Fig.12.a). The highest wear volume has been obtained for sample tested under 20 N, the volume also, decreased from 72.34 to 42.33 μm^3 with increasing sintering temperature from 950 °C to 1250 °C, respectively.

Fig.12.b shows the variation of the wear rates of the Co26Cr8Mo alloy. From Fig.12.b, For applied load of 2N, it can be seen that the wear rate decreases from $41.45x10^{-3}\ \mu m^3\ (N.m)^{-1}$ to $31.75x\ 10^{-3}\mu m^3\ (N.m)^{-1}$, when the sintering temperature increases from 950 to 1150°C, which corresponds to the conventional wear law. The highest wear rate has been obtained for sample tested under 20 N, the wear also, decreased from 53.41 to $49.95\ x10^{-3}\mu m^3\ (N.m)^{-1}$ with increasing sintering temperature from 950 °C to 1250 °C, respectively. The lowest wear rate was obtained for the sample sintered at 1250 °C which is about $31.75\ x10^{-3}\mu m^3\ (N.m)^{-1}$. This can be explained by the increase in microhardness which is produced by increasing the sintering temperature.

microhardness is an important characteristic because according to Archard's law of linear wear, the rate of wear is inversely proportional to the microhardness of the wear material (Zambrano et al., 2019). The microhardness values are in good accordance with the wear results. Other factors can also

contribute to the tribological behavior such as the transformation of the stable ε-Co phase which brings an improvement in the wear resistance of cobalt alloys (Balagna et al., 2012).

It has been observed that the structure and the microhardness have significant effects on the wear behavior of this alloy. Sintering at 1250 °C seems to be a good compromise to obtain reasonable mechanical properties (low porosity, high hardness) and improved tribological behavior. The Co28Cr6Mo alloys sintered at 950 , 1050 , 1150 °C have a closer wear track width and depth, on the other hand, for the sample sintered at 1250 °C, the wear volume is the minimum (Fig.12.a). According to this result, the friction resistance improved with increasing sintering temperature due to the closed porosity and grain size refinement.

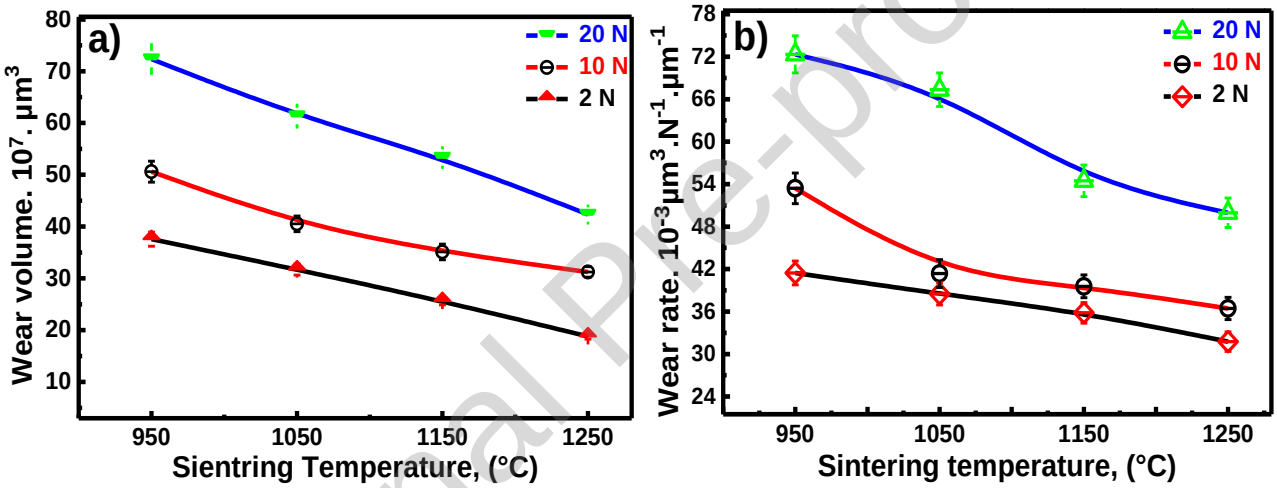

Figure 12 Evolution of: a) Wear volume (x 10^7 µm^3) and b) Wear rate (x 10^3µm^3.N^{-1}.µm^{-1}) of Co28Cr6Mo as a function of sintering temperature.

Morphological Wear track

When a surface is subjected to stresses, several varieties of warm surface can occur relying at the depth of the stresses implemented. When the latter regionally exceed the elastic restriction of one of the two substances in contact, it deforms either plastically (ductile material) or will flake of (brittle material) after a few running cycles (elasto-plastic conduct). The evaluation of the morphology and wear tracks of the sintered samples, and the ball makes it possible to discover the wear mechanisms that occur at some stage in the friction of a given couple. The micrographs obtained with a scanning electron microscope highlight the surfaces degradation mechanisms of the samples sintered at one-of-a-kind temperatures. Observations of these put on tracks display indications of abrasive and

adhesive wear mechanisms which ends up in the presence of streaks and scratches parallel to the sliding route of the Al_2O_3 ball. These phenomena are without a doubt visible on worn surfaces.

According to the SEM images (Fig. 13), it can be examined that put on debris became highlighted, which might be due to the elimination of asperities with the serve of plastic deformation or shear. Moreover, the existence of chips eliminated from the mating floor by delamination, occur, while a sufficient quantity of wear product is removed (Fig. 12. a and b). These chips may be deposited on the alumina surface or unfold over the alloy floor via the adhesive mechanism. In the case of the pattern sintered at 1150 °C (Fig.13.c), the streaks become deeper which could impact the tearing of the particles. These particles are produced by using the rupture of asperities of the floor of the material. This normally occurs in tillage put on (Stojanović et al., 2019, Lashgari et al., 2011 & Zangeneh et al., 2018).

For the sample sintered at 1250 °C (Fig.13.d), the presence of scratches parallel to the path of friction and which might be clearly seen at the worn surfaces, function of abrasive put on. It can be seen also the arrival of signs of delamination by detachment similar to adhesive put on. We will recall these mechanisms as fundamental for the touch (CoCrMo/Al_2O_3) studied.

Table 3 shows the EDS analysis and the elements present in each sample after the tribological process presented in Figure 13. The scratching made by the Alumina ball made it possible to noticeably highlight the alloying metals (Hammadi , et al., 2021). The proportions vary according to the depth of the scratch, which also depends on the hardness and resistance of each alloy and its sintering temperature (950 °C-1250 °C).

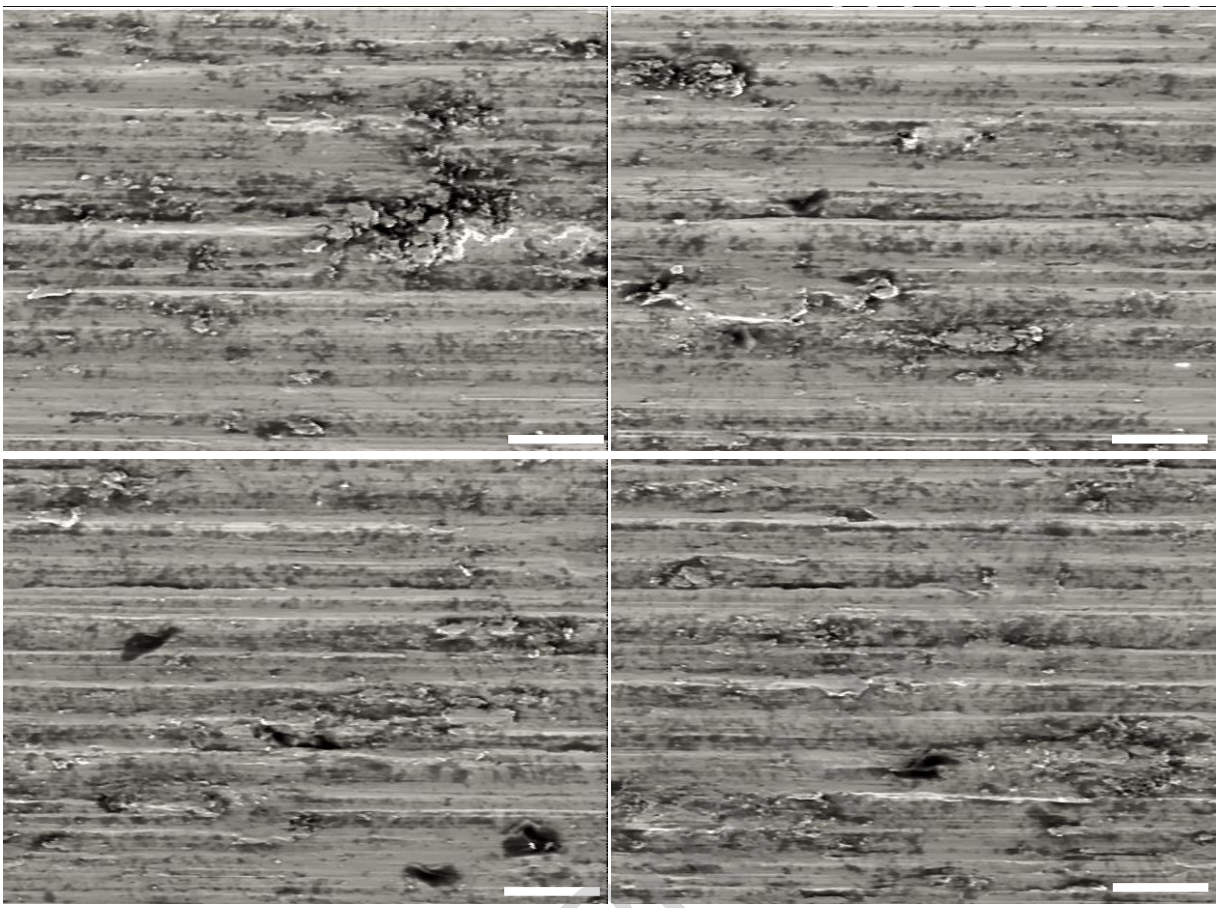

Figure 13. SEM micrographs of the wear marks formed on the surfaces of the sintered Co28Cr6Mo alloy samples: a)- 950, b)- 1100, c)- 1150 and d)- 1200 °C.

Table. 3 EDS Analysis of of the wear tracks formed on the surfaces of the sintered Co2CrMo alloy

Sample	Co (at.%)	Cr	Mo	O (at.%)
950 °C	84.05	8.6	5.05	2.3
1050 °C	77.5	14.5	4.4	3.6
1150 °C	54.7	22.6	19.2	3.5
1250 °C	61.4	25.9	8,5	4.2

CONCLUSIONS

A Co-28Cr-6Mo alloy was successfully synthesized utilizing high energy ball milling, followed by pressing and sintering at different temperatures. Structural, mechanical and tribological properties were evaluated. The following conclusions can be drawn:

- The sintered samples exhibited improved mechanical proprieties; higher densities, lower porosities, higher microhardness and stiffness with increasing sintering temperatures, due to grain refinement, atomic cohesion and closed packing.
- The morphological characterization showed the presence of one crystalline ε-hcp structure crystalline.

- Sintering, significantly enhanced structural and mechanical properties of sintered sample due to the grain size refinement.
- The enhanced microhardness had a significant contribution on improving the tribological performance of samples sintered
- The CoCrMo alloy sintered at 1250 °C gave the best structural, mechanical and tribological performances.
- The higher wear resistance of samples sintered at 1250 °C is attributed to its enhanced structural properties.
- The predominant wear mechanisms of CoCrMo alloys were found to be abrasion, adhesion And delamination defect.

Acknowledgments

- Directorate-General for Scientific Research and Technological Development (DGRSDT). For supporting this research
- Princess nourah bint Abdulrahman university researchers supporting Project number (PNURSP2023R404), princess nourah bint abdulrahman university, Riyadh, Saudi Arabia

REFERENCES

Balagna, C., Spriano, S., & Faga, M.G. 2012. Characterization of Co–Cr–Mo alloys after a thermal treatment for high wear resistance. Materials Science and Engineering C. 32(7):1868–1877.

Bouras, D., Fellah, M., Mecif, A., Barillé, R., Obrosov., A., Rasheed, M. 2023. High photocatalytic capacity of porous ceramic-based powder doped with MgO. Journal of the Korean Ceramic Society. 60: 155–168.

Cheng, Q., Zhang, P. & Ma, X. 2022. Shanhong wan microstructure evolution and wear mechanism of in situ prepared Ti–TiN cermet layers at high temperature. Composites Part B: Engineering. 242: 110028.

Corona-Gomez, J., Jack, T.A., Feng, R. & Yang, Q. 2021. Wear and corrosion characteristics of nano-crystalline tantalum nitride coatings deposited on CoCrMo alloy for hip joint applications. Materials Characterization. 182: 111516

Cuao-Moreu, C.A., Hernández-Sanchéz, E., Alvarez-Vera, M., Garcia-Sanchez, E.O., Perez-Unzueta, A. & Hernandez-Rodriguez, M.A.L. 2019. Tribological behavior of borided surface on cocrmo cast alloy. Wear. 426–427(2018): 204–211.

Eka Perkasa, D., Qonita, A. & Soegijono, B. 2019. Influence of mangan on structure and corrosion properties of cobalt chrome molybdenum (Co-Cr-Mo), IOP Conference Series: Materials Science and Engineering. 694 (1).

Fellah, M., Hezil, N., Bouras, D., Obrosov, A., Abdul Samad, M., Montagne., El Din, S., Weiß, S. 2023. Structural, Mechanical and Tribological Performance of a nano structured Biomaterial Co-Cr-Mo Alloy Synthesized Via Mechanical Alloying. Journal of Materials Research and Technology. 25: 2152-2165.

Fellah, M., Hezil, N., Bouras, D., Montagne, A., Obrosov , A., W. Ibrahim, R., Iqbal, A., El Din, S., Abd El-Wahed Khalifa, H. 2023. Investigating the effect of milling time on structural, mechanical and tribological properties of a nanostructured hiped alpha alumina for biomaterial applications. Arabian Journal of Chemistry. 16:(10)105112

Fellah, M., Hezil, N., Dekhil, L., Abdul Samad, M., Djellabi, R., Kosman, S., Montagne, A., Iost, A., Obrosov, A., Weiss, S. 2019. Effect of sintering temperature on structure and

tribological properties of nanostructured Ti–15Mo alloy for biomedical applications. Trans. Nonferrous Met. Soc. China (English Ed). 29(11): 2310–2320.

Fellah, M., Hezil, N., Touhami, M.Z., Abdul Samad, M., Obrosov, A., Bokov, D.O., Marchenko, E., Montagne, A., IOST, A., Alhussein, A. 2020. Structural, Tribological and Antibacterial Properties of (α + β) based Ti-Alloys for Biomedical Applications. Journal of Materials Research and Technology. 9(6): 14061-14074

Fellah, M., Labaïz, M., Assala, O., Dekhil, L., Taleb, A., Rezag H. & Iost, A. 2014. Tribological behavior of Ti-6Al-4V and Ti-6Al-7Nb alloys for total hip prosthesis. advances in tribology. 2014: 451387.

Fellah, M., Hezil N., A Hussein, M., Abdul Samad, M., Touhami, MZ., Montagne, A., Iost A., Obrosov, A., Weiss, S., 2019 "Preliminary investigation on the bio-tribocorrosion behaviour of porous nanostructured β-type titanium based biomedical alloy", Materials Lettres 257 : 126755,

Gong, X., Li, Y., Nie, Y., Huang, Z., Liu, F., Huang, L., Huang, L., Jiang, L. & Mei, H. 2018. Corrosion behaviour of CoCrMo alloy fabricated by electron beam melting. Corrosion Science. 139: 68–75.

Hezil, N., Fellah, M. 2019 Synthesis, structural and mechanical properties of nanobioceramic (α-Al_2O_3). 2019. Journal of the Australian Ceramic Society. 55(2019)1167-1175.

Hezil, N., Aissani, L., Fellah, M., Abdul Samad, M., Obrosov, A., Bokov, O.D, Marchenko, E. 2022. Structural, and Tribological Properties of Nanostructured α + β Type Titanium Alloys for Total Hip J. Mater. Res. Technol. 19 :3568-3578

Hammadi, F., Fellah, M., Hezil, N., Aissani, L., Mimanne, G., Mechachti, S., Abdul Samad, M., Montagne, A., Iost, A., Sabine, W., Obrosov, A. 2021. The effect of milling time on the microstructure and mechanical properties of Ti-6Al-4Fe alloys. Mater. Today Commun., 27(1): 102428

Igual Muñoz, A. & Valero Vidal, C. 2019. Influence of electrochemical conditions on cocrmo behavior in simulated body fluid by step polarization technique. Ecs transactions. 28 (24): 25–35.

Kumagai, K., Nomura, N., Ono, T., Hotta, M. & Chiba, A. 2006. Dry friction and wear behavior of forged Co-29Cr-6Mo alloy without Ni and C additions for implant applications. Nippon Kinzoku Gakkaishi/Journal of the Japan Institute of Metals. 70(4): 265–274.

Lashgari, H.R., Zangeneh, S. & Ketabchi, M. 2011. Isothermal aging effect on the microstructure and dry sliding wear behavior of Co–28Cr–5Mo–0.3C alloy. Journal of Materials Science. 46(22): 7262–7274.

Liu, Y. & Gilbert, J.L. 2017. The effect of simulated inflammatory conditions and pH on fretting corrosion of cocrmo alloy surfaces. Wear. 390 (391): 302–311.

Lizárraga, R., Pan, F., Bergqvist, L., Holmström, E., Gercsi, Z. & Vitos, L. 2017. First Principles Theory of The Hcp-Fcc Phase Transition In Cobalt. Scientific Reports. 7 (1): 6–13.

Namus, R., Rainforth, W.M., Huang, Y. & Langdon, T.G. 2020. Effect of grain size and crystallographic structure on the corrosion and tribocorrosion behaviour of a CoCrMo biomedical grade alloy in simulated body fluid. Wear. 478–479: 203884.

Ren, F., Zhu, W. & Chu, K. 2016. Fabrication, tribological and corrosion behaviors of ultra-fine grained Co-28Cr-6Mo alloy for biomedical applications. Journal of Mechanical Behavior of Biomedical Materials. 60: 139–147.

Roudnicka, M., Bigas, J., Molnarova, O., Palousek, D. & Vojtech, D. 2021. Different response of cast and 3d-printed Co-Cr-Mo alloy to heat treatment: a thorough microstructure characterization. Metals (Basel).11(5): 687.

Saldívar-García, A. & López, J.H.F. 2005. Microstructural effects on the wear resistance of wrought and As-Cast Co-Cr-Mo-C implant alloys. Journal of Biomedical Materials Research Part A. 74(2): 269–274.

Shekhawat, D., Singh, A., Bhardwaj, A. & Patnaik, A. 2021. A short review on polymer, metal and ceramic based implant materials. IOP Conference Series: Materials Science and Engineering. 1017(1).

Shukla, K., Purandare, Y., Sugumaran, A., Ehiasarian, A., Khan, I. & Hovsepian, P. 2021. Correlation between the microstructure and corrosion performance of the hipimsnitrided bio-grade cocrmo alloy. Journal of Alloys and Compounds. 879: 160429.

Sinnett-Jones, P.E., Wharton, J.A. & Wood, R.J.K. 2005. Micro-abrasion-corrosion of a cocrmo alloy in simulated artificial hip joint environments. Wear. 259 (12): 898–909.

Stojanović, B., Bauer, C., Stotter, C., Klestil, T., Nehrer, S., Franek, F. & Ripoll, M.R. 2019. Tribocorrosion of a CoCrMo alloy sliding against articular cartilage and the impact of metal ion release on chondrocytes, Acta Biomaterialia. 94: 597-609

Taghian Dehaghani, M. & Ahmadian, M. 2015. Effect of sintering temperature and time on the mechanical properties of Co–Cr–Mo/58s bioglass porous nano-composite. Bulletin of Materials Science. 38 (5): 1239–1246.

Thornley, B., Beadling, R., Bryant, M. & Neville, A. 2020. Investigation of the repassivation process of CoCrMo in simulated biological fluids. Corrosion. 76(6): 539–552.

Toh, W., Tan, X., Bhowmik, A., Liu, E. & Tor, S. 2017. Tribochemical characterization and tribocorrosive behavior of CoCrMo alloys: A Review. Materials. 11(1) :30.

Wei, D., Koizumi, Y., Takashima, T., Nagasako, M. & Chiba, A. 2018. Fatigue improvement of electron beam melting-fabricated biomedical Co–Cr–Mo alloy by accessible heat treatment. Materials Research Letters. 6(1): 93–99.

Yamanaka, K., Mori, M. & Chiba. A. 2014. Effects of nitrogen addition on microstructure and mechanical behavior of biomedical Co-Cr-Mo alloys. Journal of Mechanical Mehavior of Biomedical Materials. 29: 417–426.

Yildirim, M. & Keleş, A. 2019. Effect of aging time on phase transformation, microstructure and hardness of Co-Cr-Mo alloys. Selcuk University Journal of Engineering Science and Technology 9364: 146–153.

Yoda, K. et Al. 2012. Effects of chromium and nitrogen content on the microstructures and mechanical properties of As-Cast Co-Cr-Mo alloys for dental applications. Acta Biomaterialia. 8 (7): 2856–2862.

Zambrano, O.A., Gómez, J.A., Coronado, J.J. & Rodríguez, S.A. 2019. The sliding wear behaviour of steels with the same hardness. Wear. 418–419: 201-207.

Zangeneh, S., Lashgari, H.R. & A. Roshani. 2018. Microstructure and tribological characteristics of aged Co–28Cr–5Mo–0.3C alloy. Materials Design. 37: 292–303.

Declaration of interests

The authors declare that they have no known competing financial interests or personal relationships that could have appeared to influence the work reported in this paper.